COMPDYN 2013
4th ECCOMAS Thematic Conference on
Computational Methods in Structural Dynamics and Earthquake Engineering
M. Papadrakakis, V. Papadopoulos, V. Plevris (eds.)
Kos Island, Greece, 12–14 June 2013

STUDIES IN NUMERICAL STABILITY OF EXPLICIT CONTACT-IMPACT ALGORITHM TO THE FINITE ELEMENT SOLUTION OF WAVE PROPAGATION PROBLEMS

Ján Kopačka[1], Dušan Gabriel[1], Radek Kolman[1], Jiří Plešek[1] and Miran Ulbin[2]

[1]Institute of Thermomechanics, Academy of Sciences
Dolejškova 5, 182 00 Prague 8, Czech Republic
e-mail: {gabriel,kopacka,kolman,plesek}@it.cas.cz

[2] Faculty of Mechanical Engineering, University of Maribor
Smetanova 17, 2000 Maribor, Slovenia
e-mail: ulbin@uni-mb.si

Keywords: Contact-impact, central difference method, stability, penalty method, bipenalty method.

Abstract.

In dynamic transient analysis, recent comprehensive studies have shown that using mass penalty together with standard stiffness penalty, the so-called bipenalty technique, preserves the critical time step in conditionally stable time integration schemes. In this paper, the bipenalty approach is applied in the explicit contact-impact algorithm based on the pre-discretization penalty formulation. The attention is focused on the stability of this algorithm. Specifically, the upper estimation of the stable Courant number on the stiffness and mass penalty is derived based on the simple dynamic system with two degrees-of-freedom. The results are verified by means of the dynamic Signorini problem, which is represented by the motion of a bar that comes into contact with a rigid obstacle.

1 INTRODUCTION

In contact problems the contact constraints can be enforced either by the Lagrange multiplier method or by the stiffness penalty method. In practise the latter approach has gained in substantial popularity, because its implementation is easy, straightforward and has a clear physical meaning. On the other hand, the choice of the penalty parameter influences the accuracy of the approximate solution. In addition, in contact-impact applications the stiffness penalty method tends to decrease the critical time step in conditionally stable time integration schemes. This is due to the fact that the stiffness-type penalty can greatly enlarge the maximum eigenfrequency of a system.

In dynamic transient analysis, the penalty method can also be applied to the mass matrix. This technique is known as the mass penalty or the inertia penalty method. In contrast to the stiffness penalty approach, it significantly reduces one or more eigenfrequencies. In Reference [1] the bipenalty technique was introduced, where the both penalty formulations were used simultaneously. The goal of this method is to find the optimum of the so-called critical penalty ratio (CPR) defined as the ratio of stiffness and mass penalty parameters so that the maximum eigenfrequency and the critical time step are preserved. The calculation of CPR requires an analysis of the full bipenalised problem. Owing to mathematical difficulty, it limits the classes of elements that can be taken into account. In order to overcome this problem, a simple relationship between the CPR of an element and its maximum unpenalised eigenfrequency was derived in [2]. Thus, the multiple constraints and more complex element formulations can be directly accounted for [3].

In this paper, the bipenalty approach is applied in the explicit contact-impact algorithm based on the pre-discretization penalty formulation [4]. The attention is focused on the stability properties of this algorithm. In Section 2.1 the formulation of contact initial/boundary value problem is presented, followed by the variational formulation in Section 2.2. The idea of the bipenalty approach for imposing the contact constraints is described in Section 2.3. Finite element discretization is outlined in Section 2.4. The numerical stability of explicit time integration scheme is discussed in Section 2.5. Based on the behaviour of the simple dynamic system with two degrees-of-freedom the upper estimation of the stable Courant number on the stiffness and mass penalty is derived. In Section 3, the stability of the algorithm is tested on the dynamic Signorini problem, followed by concluding remarks in Section 4.

2 PROBLEM DESCRIPTION

2.1 Contact initial/boundary value problem

The problem of linear elastodynamics is governed by the balance of linear momentum

$$\boldsymbol{\nabla} \cdot \boldsymbol{\sigma}(\mathbf{u}) + \mathbf{b} = \rho \ddot{\mathbf{u}}(\mathbf{x}, t) \quad \text{in } \Omega \times \mathbb{I} \tag{1}$$

where $\Omega = \bigcup_i \Omega_i, i = 1, 2$ is n-dimensional set of spatial points, $\mathbf{x} \in \mathbb{R}^n$, defining the contacting bodies, $\mathbb{I} = (0, T)$ is the time domain, $\mathbf{u}$ is the displacement field, $\boldsymbol{b}$ are the body forces and $\boldsymbol{\sigma}$ is the stress field (see Figure 1). The superimposed dots denote the time derivatives. In linear elasticity the stress can be computed from the linear strain field

$$\boldsymbol{\varepsilon} = \frac{1}{2}\left((\boldsymbol{\nabla}\mathbf{u})^{\mathrm{T}} + \boldsymbol{\nabla}\mathbf{u}\right) \tag{2}$$

via Hooke's law

$$\boldsymbol{\sigma} = \mathbf{c} : \boldsymbol{\varepsilon} \tag{3}$$

where $\mathbf{c}$ is the tensor of elastic constants given as

$$\mathbf{c} = \lambda \mathbf{I} \otimes \mathbf{I} + 2\mu \mathbf{I} \tag{4}$$

where $\mathbf{I}$ is the second-order identity tensor and λ, μ are the Lamé constants. The problem is in general subject to certain initial and boundary conditions as well. The initial conditions

$$\mathbf{u}(\mathbf{x}, 0) = \mathbf{u}_0 \quad \text{in } \bar{\Omega} \tag{5}$$
$$\dot{\mathbf{u}}(\mathbf{x}, 0) = \mathbf{v}_0 \quad \text{in } \bar{\Omega} \tag{6}$$

are prescribed in the closure of domain $\bar{\Omega}$. The displacement and traction boundary conditions

$$\mathbf{u} = \bar{\mathbf{u}} \quad \text{on } \Gamma_{\mathrm{u}} \tag{7}$$
$$\boldsymbol{\sigma} \cdot \mathbf{n} = \bar{\mathbf{t}} \quad \text{on } \Gamma_{\sigma} \tag{8}$$

are prescribed on the $\Gamma_{\mathrm{u}} \subset \Gamma$ and $\Gamma_{\sigma} \subset \Gamma$, respectively; Γ denotes the boundary of the domain Ω; $\bar{\mathbf{u}}$ and $\bar{\mathbf{t}}$ are the prescribed displacements and the prescribed tractions, respectively; the vector $\mathbf{n}$ stands for the outward normal vector to Γ_{σ}. Further, the contact constraints are described on the contact boundary $\Gamma_{\mathrm{c}} \subset \Gamma$ by the Signorini-Hertz-Moreau conditions

$$g_{\mathrm{N}} \geq 0 \quad t_{\mathrm{N}} = \boldsymbol{\sigma} \cdot \mathbf{n} \leq 0 \quad g_{\mathrm{N}} t_{\mathrm{N}} = 0 \quad \text{on } \Gamma_{\mathrm{c}} \tag{9}$$

also known as the Karush-Kuhn-Tucker (KKT) conditions. Here, the normal gap function g_{N} has been introduced, which is defined as

$$g_{\mathrm{N}} = \begin{cases} (\mathbf{x}_2 - \bar{\mathbf{x}}_1) \cdot \bar{\mathbf{n}}_1 & \text{if } (\mathbf{x}_2 - \bar{\mathbf{x}}_1) \cdot \bar{\mathbf{n}}_1 < 0 \\ 0 & \text{otherwise} \end{cases} \tag{10}$$

The definition is apparent from Figure 1, where $\bar{\mathbf{x}}_1$ is the closest point projection of the point $\mathbf{x}_2$, lying on the contact boundary of body Ω_2, onto the contact boundary of body Ω_1. The vector $\bar{\mathbf{n}}$ denotes the contact normal vector.

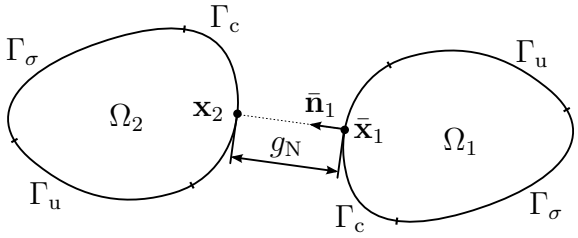

Figure 1: Definition of the normal gap function.

The first inequality $(9)_1$ is called the impenetrability condition. The second condition $(9)_2$ asserts the negative traction vector on the contact boundary. And finally, the third equality $(9)_3$ is called the complementarity condition ensuring the complementarity between the gap function and the contact traction vector.

2.2 Variational formulation

In order to be able to perform the finite element discretization, it is necessary to reformulate the strong form of the contact initial/boundary value problem presented in the preceding section in a weak sense. Hamilton's principle is a simple and powerful tool that can be utilised to derive discretized dynamic system of equations. It states that of all admissible time histories of displacement field the solution is one which minimizes the action functional

$$\mathbf{u} = \arg\min \left(\int_0^T \mathcal{L}\left(\mathbf{u}, \dot{\mathbf{u}}\right) \, \mathrm{d}t \right) \quad \text{subjected to } g_{\mathrm{N}} \geq 0 \text{ on } \Gamma_{\mathrm{c}} \tag{11}$$

where the Lagrangian functional, $\mathcal{L}(\mathbf{u}, \dot{\mathbf{u}})$, is defined as

$$\mathcal{L}\left(\mathbf{u}, \dot{\mathbf{u}}\right) = \mathcal{T}\left(\dot{\mathbf{u}}\right) - \left(\mathcal{U}\left(\mathbf{u}\right) - \mathcal{W}\left(\mathbf{u}\right)\right) \tag{12}$$

where

$$\mathcal{T}\left(\dot{\mathbf{u}}\right) = \int_\Omega \frac{1}{2} \rho \dot{\mathbf{u}} \cdot \dot{\mathbf{u}} \, \mathrm{d}V \tag{13}$$

$$\mathcal{U}\left(\mathbf{u}\right) = \int_\Omega \frac{1}{2} \boldsymbol{\sigma} : \boldsymbol{\varepsilon} \, \mathrm{d}V \tag{14}$$

$$\mathcal{W}\left(\mathbf{u}\right) = \int_\Omega \mathbf{u} \cdot \mathbf{b} \, \mathrm{d}V + \int_{\Gamma_\sigma} \mathbf{u} \cdot \bar{\mathbf{t}} \, \mathrm{d}S \tag{15}$$

are the kinetic energy, the strain energy, and the work done by external forces, respectively.

2.3 Bipenalty method

In dynamics, the simultaneous use of the stiffness penalties and inertia/mass penalties, called the bipenalty method, was originally proposed in [1]. There was defined the penalty ratio as

$$R = \frac{\epsilon_{\mathrm{s}}}{\epsilon_{\mathrm{m}}} \left[\mathrm{s}^{-2}\right] \tag{16}$$

where ϵ_{s} and ϵ_{m} are the stiffness and mass penalty parameter, respectively. There were also derived optimum values of the penalty ratios–the so-called critical penalty ratios (CPR)–for a number of finite elements such that the critical time step of the penalised system remains unaffected. A new method of calculating the CPR associated with a finite element formulation was developed in [2]. Recently, this finding was extended to include systems with an arbitrary set of multipoint constraints [3].

Now, a brief description of the bipenalty method follows. Let us assume that the contact boundary Γ_{c} is known. The standard stiffness penalty method adds an extra term to the strain energy (14) to enforce the zero gap on the contact boundary

$$\mathcal{U}_{\mathrm{p}}\left(\mathbf{u}\right) = \int_\Omega \frac{1}{2} \boldsymbol{\sigma} : \boldsymbol{\varepsilon} \, \mathrm{d}V + \int_{\Gamma_{\mathrm{c}}} \frac{1}{2} \epsilon_{\mathrm{s}} g_{\mathrm{N}}^2 \, \mathrm{d}S \tag{17}$$

Further, the inertia penalty term can also be added to the kinetic energy (13) to enforce the zero gap rate on the contact interface

$$\mathcal{T}_{\mathrm{p}}\left(\dot{\mathbf{u}}\right) = \int_\Omega \frac{1}{2} \rho \dot{\mathbf{u}} \cdot \dot{\mathbf{u}} \, \mathrm{d}V + \int_{\Gamma_{\mathrm{c}}} \frac{1}{2} \epsilon_{\mathrm{m}} \dot{g}_{\mathrm{N}}^2 \, \mathrm{d}S \tag{18}$$

Now, a new penalised Lagrangian functional can be defined as

$$\mathcal{L}_{\mathrm{p}}(\mathbf{u}, \dot{\mathbf{u}}) = \mathcal{T}_{\mathrm{p}}(\dot{\mathbf{u}}) - (\mathcal{U}_{\mathrm{p}}(\mathbf{u}) - \mathcal{W}(\mathbf{u})) \tag{19}$$

The unknown displacement field can be found as one which renders the penalised action functional stationary

$$\delta \int_0^T \mathcal{L}_{\mathrm{p}}\left(\mathbf{u}, \dot{\mathbf{u}}\right)\, \mathrm{d}t = 0 \tag{20}$$

where δ denotes the first variation or the directional derivative in the direction of virtual displacement $\delta\mathbf{u}$. Using the standard procedures one arrives to the principle of virtual displacement

$$\int_\Omega \rho\delta\mathbf{u}\cdot\ddot{\mathbf{u}}\,\mathrm{d}V + \int_\Omega \delta\boldsymbol{\varepsilon} : \boldsymbol{\sigma}\,\mathrm{d}V + \int_{\Gamma_{\mathrm{c}}} \delta g_{\mathrm{N}}(\epsilon_{\mathrm{m}}\ddot{g}_{\mathrm{N}} + \epsilon_{\mathrm{s}} g_{\mathrm{N}})\,\mathrm{d}S = \int_\Omega \delta\mathbf{u}\cdot\mathbf{b}\,\mathrm{d}V + \int_{\Gamma_\sigma} \delta\mathbf{u}\cdot\mathbf{t}\,\mathrm{d}S \tag{21}$$

which serves the base for the finite element discretization. The integrals in Equation (21) represent the virtual work of the inertia forces, internal forces, contact forces, body forces, and traction forces, respectively. It is worth noting that the integral of the virtual contact work are expressed with the aid of the inertia and the stiffness penalty.

2.4 Finite element method

Applying the finite element discretization to the variational formulation (21) introduces the system of nonlinear ordinary differential equations

$$\mathbf{M}\ddot{\mathbf{u}} + \mathbf{K}\mathbf{u} + \mathbf{R}_{\mathrm{c}}(\mathbf{u}, \ddot{\mathbf{u}}) = \mathbf{R} \tag{22}$$

Here, $\mathbf{M}$ is the mass matrix, $\mathbf{K}$ is the stiffness matrix, $\mathbf{R}_{\mathrm{c}}$ is the contact residual vector, which is the source of the nonlinearity. Further, $\mathbf{R}$ is the time-dependent load vector, and $\mathbf{u}$ and $\ddot{\mathbf{u}}$ contain nodal displacements and accelerations, respectively. The element mass and stiffness matrices are given by

$$\mathbf{M}_e = \int_{\Omega_e} \rho\mathbf{H}^{\mathrm{T}}\mathbf{H}\,\mathrm{d}V \qquad \mathbf{K}_e = \int_{\Omega_e} \mathbf{B}^{\mathrm{T}}\mathbf{C}\mathbf{B}\,\mathrm{d}V \tag{23}$$

where $\mathbf{C}$ it the elasticity matrix, $\mathbf{B}$ is the strain-displacement matrix, and $\mathbf{H}$ stores the shape functions. Note that the integration is carried over the element domain Ω_e. Global matrices are assembled in the usual fashion.

In the case of geometrically linear kinematics, the contact residual vector can be written as

$$\mathbf{R}_{\mathrm{c}}(\mathbf{u}, \ddot{\mathbf{u}}) = \mathbf{M}_{\mathrm{p}}\ddot{\mathbf{u}} + \mathbf{K}_{\mathrm{p}}\mathbf{u} + \mathbf{f}_{\mathrm{p}} \tag{24}$$

where

$$\mathbf{M}_{\mathrm{p}} = \int_{\Gamma_{\mathrm{c}}} \epsilon_{\mathrm{m}}\mathbf{N}\mathbf{N}^{\mathrm{T}}\,\mathrm{d}S \qquad \mathbf{K}_{\mathrm{p}} = \int_{\Gamma_{\mathrm{c}}} \epsilon_{\mathrm{s}}\mathbf{N}\mathbf{N}^{\mathrm{T}}\,\mathrm{d}S \qquad \mathbf{f}_{\mathrm{p}} = \int_{\Gamma_{\mathrm{c}}} \epsilon_{\mathrm{s}}\mathbf{N} g_0\,\mathrm{d}S \tag{25}$$

Here, $\mathbf{M}_{\mathrm{p}}$ is the additional mass matrix due to inertia penalty, $\mathbf{K}_{\mathrm{p}}$ is the additional stiffness matrix due to stiffness penalty, and $\mathbf{f}_{\mathrm{p}}$ is the part of the contact force due to the initial gap g_0. The matrix $\mathbf{N}$ represents an operator from the displacement field $\mathbf{u}$ to the gap function g_{N}

$$g_{\mathrm{N}} = \mathbf{N}^{\mathrm{T}}\mathbf{u} + g_0 \tag{26}$$

The particular form of the matrix $\mathbf{N}$ follows from the used contact discretization. A comprehensive overview can be found in [5].

2.5 Explicit time integration and numerical stability

We now consider the time integration of the semi-discretized system (22) by the central difference method (CDM) [7]

$$(\mathbf{M}+\mathbf{M}_{\mathrm{p}}^{t})\frac{\mathbf{u}^{t+\Delta t}-2\mathbf{u}^{t}+\mathbf{u}^{t-\Delta t}}{\Delta t^{2}}+(\mathbf{K}+\mathbf{K}_{\mathrm{p}}^{t})\mathbf{u}^{t}+\mathbf{f}_{\mathrm{p}}^{t}-\mathbf{R}^{t}=\mathbf{0} \tag{27}$$

Assuming that displacements are known at time $t-\Delta t$ and t, one can resolve unknown displacements at time $t+\Delta t$. Note that the matrices $\mathbf{M}_{\mathrm{p}}^{t}$ and $\mathbf{K}_{\mathrm{p}}^{t}$ are time-dependent because they are associated with active contact constraints. This fact causes the system to be nonlinear.

It is well known that the CDM for a linear system is conditionally stable. The linear stability theory establishes the upper bound of the time step as

$$\Delta t \leq \frac{2}{\omega_{\max}} \tag{28}$$

where $\omega_{\max}$ is the maximum eigenfrequency of the finite element mesh. Indeed, the computation of even a single eigenvalue of a large systems may be expensive. Therefore, it would be advantageous to have an estimate on the maximum eigenvalue that is easy to compute. Such an estimate is provided by the element eigenvalue inequality [7]

$$\omega_{\max} < \max_{e} \omega_{\max}^{e} \tag{29}$$

Note that the element eigenvalue inequality is not limited only to element level submatrices. The submatrices may be also an assemblage of elements.

Unfortunately, there are no stability theorems for contact-impact problems [7]. In this case the linear stability theory can be applied carefully. In practise, for example, the stability may be preserved by checking the energy balance during a nonlinear computation. In Reference [8] an upper bound for the stiffness penalty was derived. Moreover, it was shown that the stiffness penalty always decreases the stable time step. In this work, we generalize this estimate for the bipenalty approach following the Belytschko approach [8].

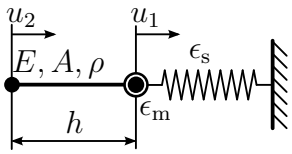

Figure 2: A simple dynamic system with two degrees-of-freedom.

Let us consider a simple dynamic system, depicted in Figure 2, with two degrees-of-freedom. The system consists of one 1D constant strain truss element with lumped mass matrix. The active contact constraint is set in node 1. The aim is to determine the maximum eigenfrequency of this system to estimate the stable time step in the form (28). To this end, the eigenvalue problem can be formulated as

$$\frac{EA}{h}\begin{bmatrix} 1+\beta_{\mathrm{s}} & -1 \\ -1 & 1 \end{bmatrix}\mathbf{u}=\omega^{2}\frac{\rho Ah}{2}\begin{bmatrix} 1+\beta_{\mathrm{m}} & 0 \\ 0 & 1 \end{bmatrix}\mathbf{u} \tag{30}$$

where the dimensionless mass and stiffness penalty have been introduced as

$$\beta_{\mathrm{m}} = \frac{2}{\rho A h}\epsilon_{\mathrm{m}} \quad \beta_{\mathrm{s}} = \frac{h}{EA}\epsilon_{\mathrm{s}} \tag{31}$$

The maximum eigenfrequency of the problem (30) is given by

$$\omega_{\max} = \frac{c_0}{h}\sqrt{1 + \frac{(1+\beta_{\mathrm{s}})}{(1+\beta_{\mathrm{m}})} + \sqrt{1 + \frac{(1+\beta_{\mathrm{s}})^2}{(1+\beta_{\mathrm{m}})^2} + \frac{2(1-\beta_{\mathrm{s}})}{(1+\beta_{\mathrm{m}})}}} \tag{32}$$

The Courant dimensionless number is defined as

$$C_{\mathrm{r}} = \frac{c_0 \Delta t}{h} \tag{33}$$

Substituting (32) into (28) using (33) the upper bound of the stable Courant number for the bipenalty method is obtained

$$C_{\mathrm{r}} = \frac{2}{\sqrt{1 + \frac{(1+\beta_{\mathrm{s}})}{(1+\beta_{\mathrm{m}})} + \sqrt{1 + \frac{2(1-\beta_{\mathrm{s}})}{(1+\beta_{\mathrm{m}})} + \frac{(1+\beta_{\mathrm{s}})^2}{(1+\beta_{\mathrm{m}})^2}}}} \tag{34}$$

Now, it is useful to introduce a new dimensionless penalty ratio r as

$$r = \frac{1}{2}\frac{\beta_{\mathrm{s}}}{\beta_{\mathrm{m}}} = \frac{h^2}{4c_0^2}R \tag{35}$$

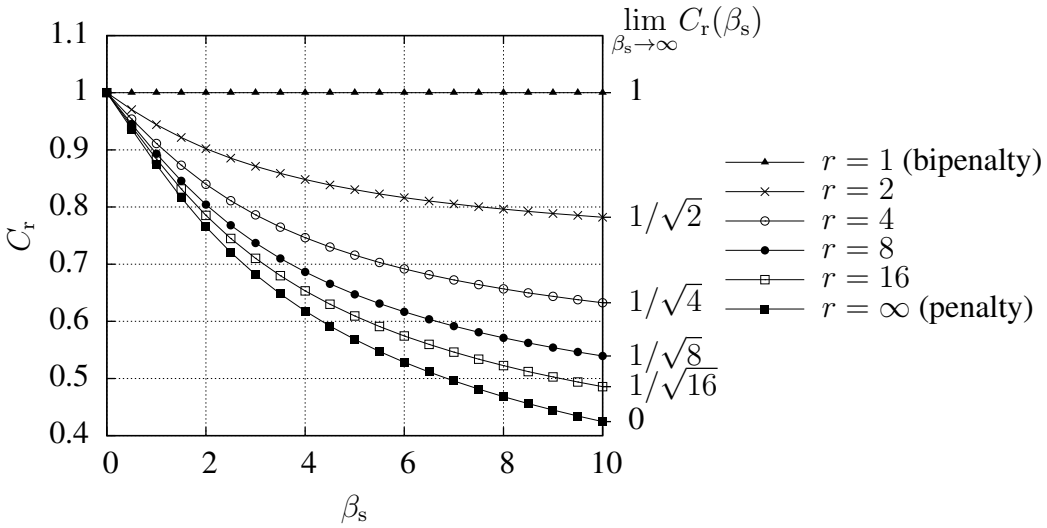

Figure 3: The dependence of the Courant number C_{r} on the dimensionless stiffness penalty β_{s} for selected dimensionless penalty ratios r.

The dependence of the Courant number C_{r} on the dimensionless stiffness penalty β_{s} is plotted in Figure 3, where the dimensionless penalty ratio r is employed as the parameter. The curve

for $r \to \infty$ (i.e. $\beta_{\mathrm{m}} \to 0$) corresponds to the standard stiffness penalty method. It illustrates the main disadvantages of the standard stiffness penalty method: the Courant number C_{r} rapidly decrease with increasing dimensionless stiffness penalty β_{s}. On the other hand, the curve for $r = 1$ confirms the existence of the CPR, for which the stable time step remains unchanged for an arbitrary value of the dimensionless stiffness penalty β_{s}. In addition, there are more curves in Figure 3 for dimensionless penalty ratios $r = 2, 4, 8,$ and 16. For each of them, there are limits of the Courant number for $\beta_{\mathrm{s}} \to \infty$ on the right edge of the picture. It is clear that the bipenalty method with the penalty ratio equal to the CPR is superior over the standard stiffness penalty method.

3 NUMERICAL EXAMPLE

In this section, the stability of explicit contact-impact algorithm using bipenalty technique was studied on the dynamic Signorini problem, which was represented by the motion of a bar that comes into contact with a rigid obstacle (see Figure 4). The bar of length $L = 1\,[\mathrm{m}]$ with the initial velocity $v_0 = 1\,[\mathrm{m} \cdot \mathrm{s}^{-1}]$ is situated at distance of $g_0 = 0\,[\mathrm{m}]$ in front of the obstacle. The area of the bar section $A\,[\mathrm{m}^2]$, Young's modulus $E\,[\mathrm{MPa}]$ and density $\rho\,[\mathrm{kg} \cdot \mathrm{m}^{-3}]$ were chosen to be unit.

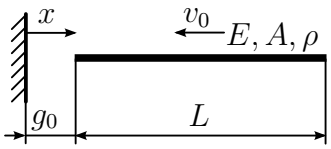

Figure 4: 1D dynamic Signorini problem.

The bar was discretized by a regular finite element mesh containing one hundred 1D constant strain truss elements. For the effective integration of equilibrium equations by the CDM method the consistent mass matrix was diagonalized by the row sum technique. The maximum eigenvalue of the mesh was $\lambda_{\max} = 4e4\,[\mathrm{s}^{-2}]$ and the corresponding eigenfrequency was $\omega_{\max} = 200\,[\mathrm{s}^{-1}]$.

Let us introduce following dimensionless quantities

$$t^* = \frac{c_0 t}{L} \qquad x^* = \frac{x}{L} \qquad u^* = \frac{u(0,t)}{L} \qquad F_{\mathrm{c}}^* = \frac{c_0 F_{\mathrm{c}}}{v_0 E A} \qquad \sigma^* = \frac{\sigma A}{F_{\mathrm{c}}} \tag{36}$$

where $t^*, x^*, u^*, F_{\mathrm{c}}^*, \sigma^*$ is the dimensionless time, coordinate, contact displacement, contact force, stress, respectively. In the following figures, the results for the standard penalty method (left) and the bipenalty method (right) are plotted.

The dimensionless stiffness penalty β_{s} was chosen to 1.5. In order to verify derived formula of the stability (34) the Courant number C_{r} was set to 0.82, which was slightly higher than the critical value $C_{\mathrm{r}} = 0.81649658$ for the penalty method. The results are shown in Figure 5a, where time distributions of the kinetic energy, the potential energy, the total energy, the work done by contact forces are plotted. It was confirmed that the stability of the CDM was lost for the penalty method, whereas the solution obtained by the bipenalty method still perfectly conserved the total energy. When the Courant number C_{r} was set to 0.5 both methods were stable (see Figure 6).

Note that the work of contact force W_{c} is almost zero. In fact, it should be exactly zero because the displacement of the contact force was restricted by the rigid obstacle. However, in

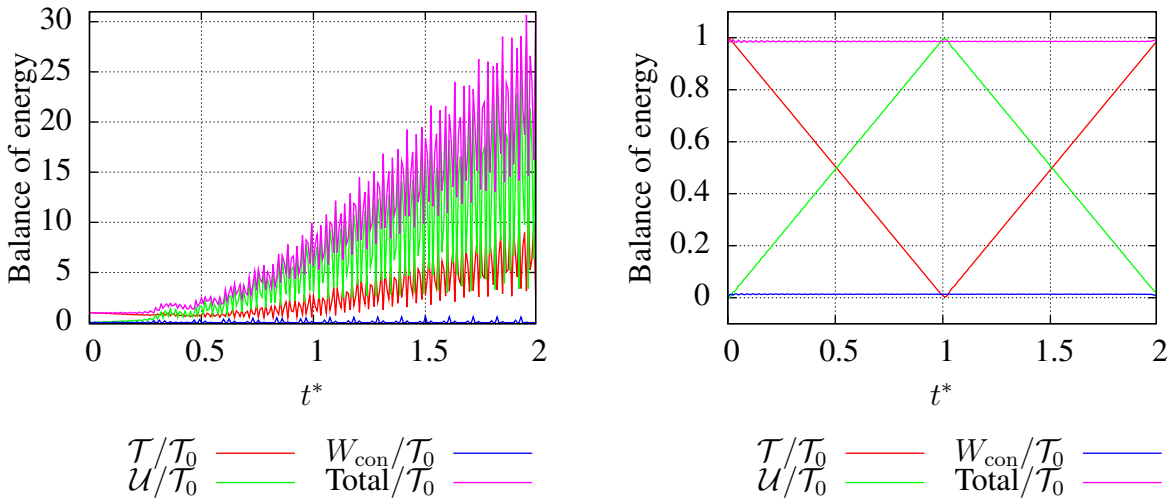

(a) $r = \infty$ (penalty method) (b) $r = 1$ (bipenalty method)

Figure 5: Time distribution of the balance of energy for $\beta_{\text{s}} = 1.5$ and $C_{\text{r}} = 0.82$.

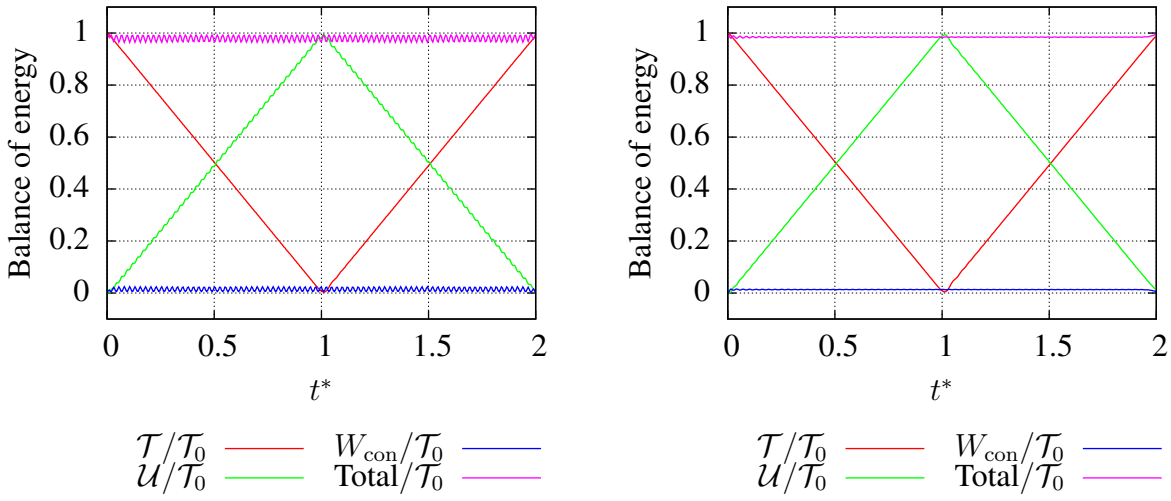

(a) $r = \infty$ (penalty method) (b) $r = 1$ (bipenalty method)

Figure 6: Time distribution of the balance of energy for $\beta_{\text{s}} = 1.5$ and $C_{\text{r}} = 0.5$.

the penalty-like methods, contact forces perform a spurious work on penetrations. This work converges to zero as β_{s} tends to infinity. Nevertheless, a finite value of the stiffness penalty parameter always results in a non-zero work of contact force. One can also notice the presence of oscillations in the distributions of the potential energy and the work of contact forces, which result in oscillations in the distributions of the total energy. This phenomenon is primarily caused by the oscillations in the gap function, which will be discussed further.

Figure 7 shows time distribution of the dimensionless contact displacement for $\beta_{\text{s}} = 1.5$ and $C_{\text{r}} = 0.5$. The gap should be equal to zero during the impact, which is indicated by the exact solution in the Figure 7. It is well known that penalty-like methods allow certain

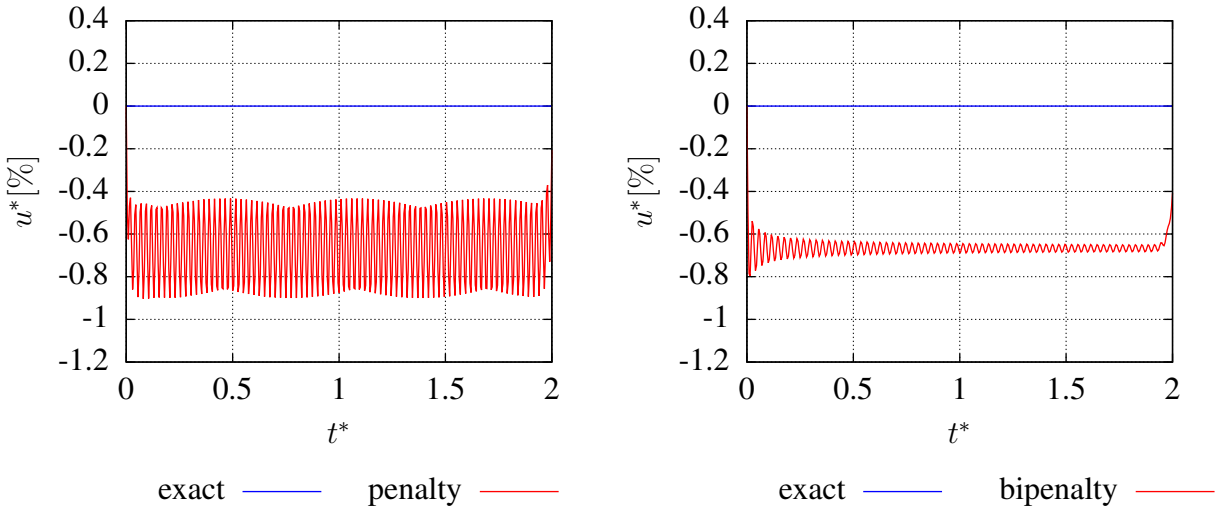

(a) $r = \infty$ (penalty method)

(b) $r = 1$ (bipenalty method)

Figure 7: Time distribution of the dimensionless contact displacement for $\beta_s = 1.5$ and $C_r = 0.5$.

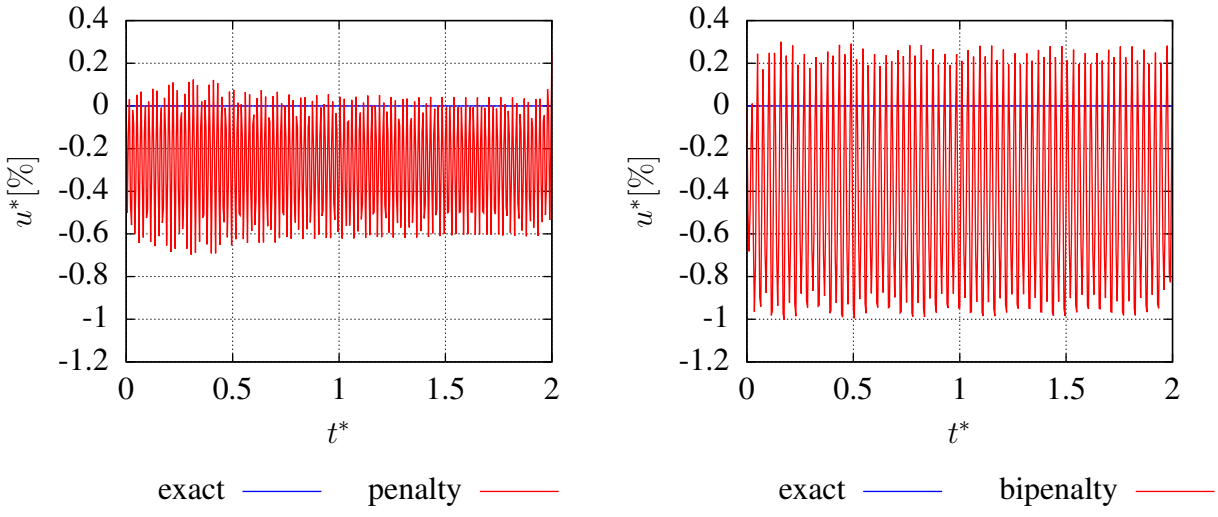

(a) $r = \infty$ (penalty method)

(b) $r = 1$ (bipenalty method)

Figure 8: Time distribution of the dimensionless contact displacement for $\beta_s = 3.5$ and $C_r = 0.5$.

penetration of contact interfaces. As a result, the oscillations of kinematic and stress quantities can occur in impact problems. Figure 7b displays an attenuation of the oscillations for the bipenalty approach in comparison with the penalty method. However, from a certain value of the dimensionless stiffness penalty β_s it was observed that the amplitude of oscillations were even higher for the bipenalty method than for the penalty method. An example is shown in Figure 8, where $\beta_s = 3.5$ was considered. The reason probably is that the oscillation of the contact displacement overshot zero value. Thus, the contact constraint was deactivated and the

contact force disappeared. In consequent iterations, the contact constraint was again activated. Therefore, the system was switching between two states which generated the oscillations.

This phenomenon can also be observed in Figure 10, where time distribution of the dimensionless contact force is plotted. Both distributions are bounded by zero value. On the other hand, for the previously chosen value of dimensionless stiffness penalty $\beta_s = 1.5$ time dependence of of the dimensionless contact force oscillated around the exact solution as indicated in Figure 9. Similarly to distribution of the contact displacement in Figure 7b the bipenalty method dumped oscillations in the distribution of contact force depicted in Figure 9b.

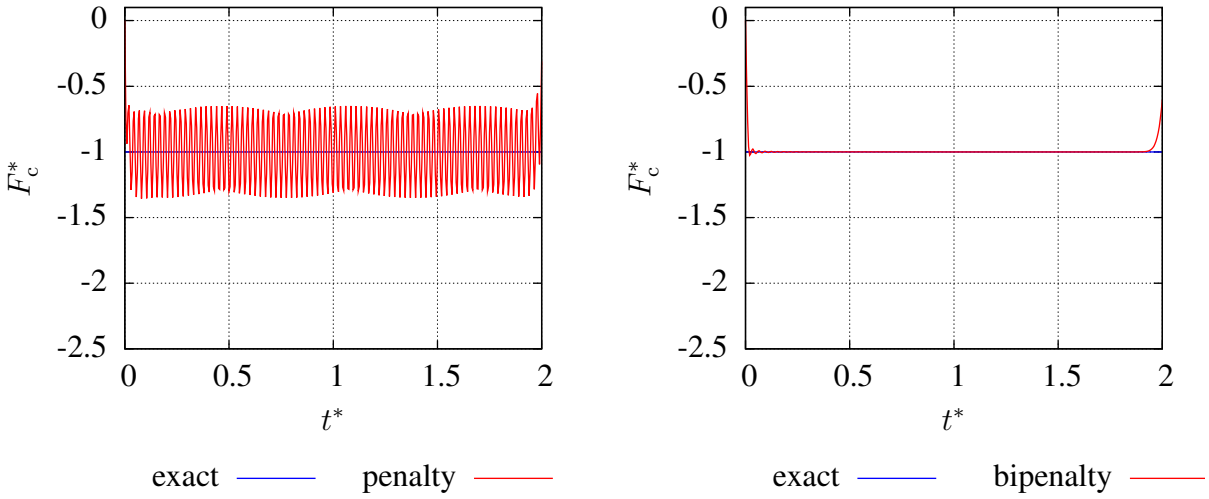

(a) $r = \infty$ (penalty method) (b) $r = 1$ (bipenalty method)

Figure 9: Time distribution of the dimensionless contact force for $\beta_s = 1.5$ and $C_r = 0.5$.

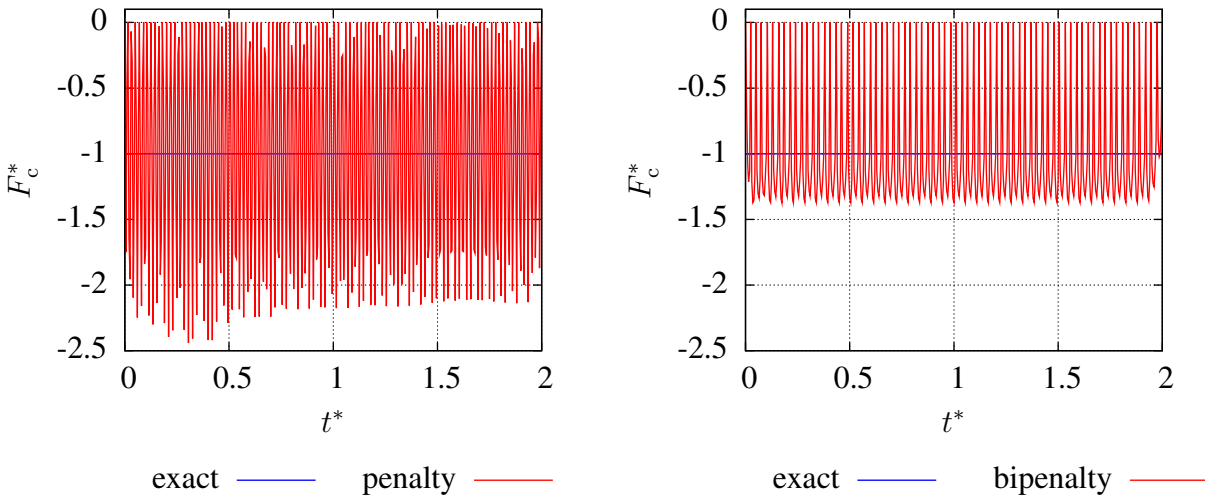

(a) $r = \infty$ (penalty method) (b) $r = 1$ (bipenalty method)

Figure 10: Time distribution of the dimensionless contact force for $\beta_s = 3.5$ and $C_r = 0.5$.

Figure 11 shows spatial distribution stress along the bar when the wavefront reached a half of the bar. In addition to contact analysis, a reference calculation was performed, where the axial displacement of the contact node was fixed.

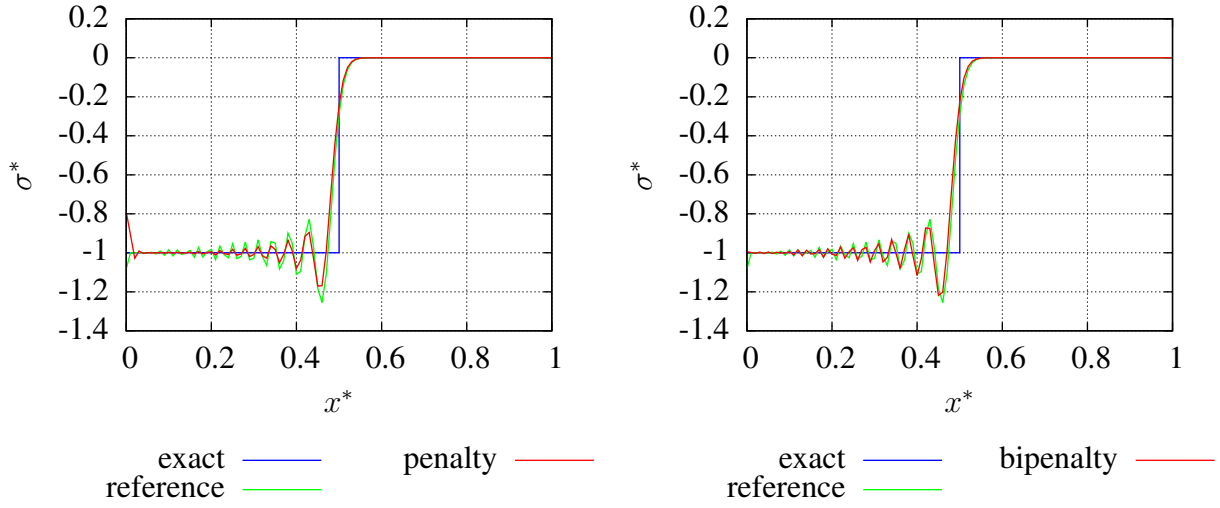

(a) $r = \infty$ (penalty method) (b) $r = 1$ (bipenalty method)

Figure 11: Spatial distribution of the dimensionless stress for $\beta_s = 1.5$ and $C_r = 0.5$.

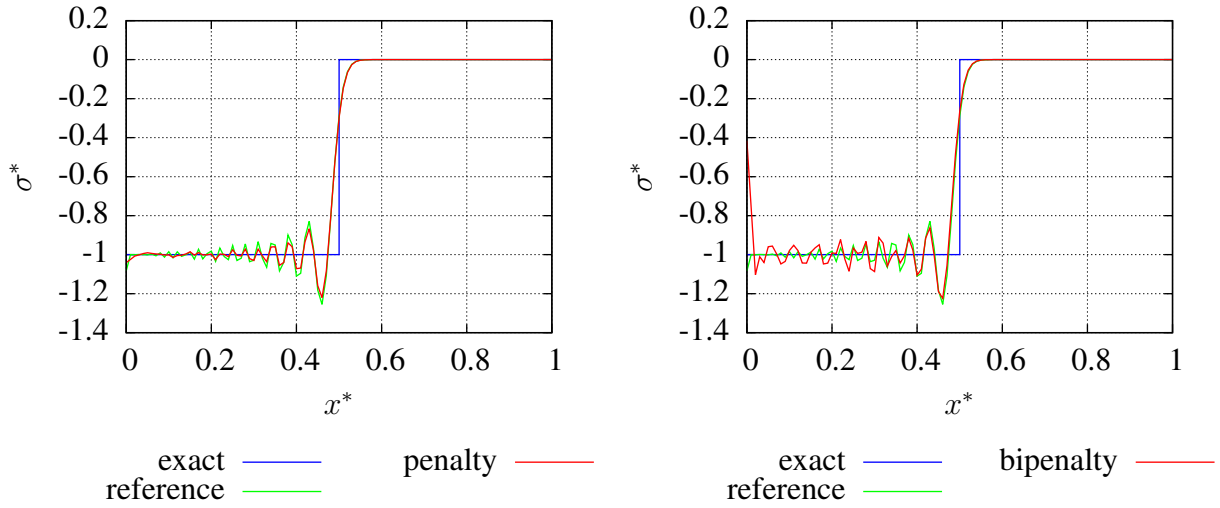

(a) $r = \infty$ (penalty method) (b) $r = 1$ (bipenalty method)

Figure 12: Spatial distribution of the dimensionless stress for $\beta_s = 3.5$ and $C_r = 0.5$.

Stress distributions for both the penalty and the bipenalty method was in a good agreement with the reference solution (see Figures 11 and 12). The reason probably is that the finite element mesh behaves as a low-pass filter [9] and therefore high frequency oscillations introduced by the penalty-like methods do not affect the solution.

4 CONCLUSIONS

In this paper, the stability of explicit contact-impact algorithm [4] using the bipenalty approach was studied. The upper bound of the stable Courant number on the stiffness penalty and mass penalty was derived based on the simple dynamic system with two degrees-of-freedom. It was shown that the critical Courant number tend towards zero for the stiffness penalty approaching infinity whereas the mass penalty was considered to be zero. On the other hand, when the penalty ratio was set to the critical value CPR, which corresponded to the maximum eigenvalue of the unpenalised system, the critical Courant number was equal to one for the arbitrary value of the stiffness penalty.

The derived upper bound of the stability was verified by means of the simple 1D dynamic Signorini problem. It was demonstrated decreasing the critical time step for the standard penalty method and its preserving for the bipenalty method. The example also revealed that both methods caused spurious oscillations in the distributions of displacement and the contact force. This effect was especially obvious for higher values of stiffness penalty parameters. The estimation of the penalty parameter ensuring non-oscillated behaviour of both methods will be investigated in further work.

5 ACKNOWLEDGEMENTS

Support by ME10114, GAP101/12/2315 and GA101/09/1630 with institutional support RVO:61388998 is acknowledged.

REFERENCES

[1] H. Askes, M. Caramés-Saddler, A. Rodriguez-Ferran, Bipenalty method for time domain computational dynamics. *Proceedings of the Royal Society A: Mathematical, Physical and Engineering Sciences*, **466**, 1389–1408, 2010.

[2] J. Hetherington, A. Rodriguez-Ferran, H. Askes, A new bipenalty formulation for ensuring time step stability in time domain computational dynamics. *International Journal for Numerical Methods in Engineering*, **90**, 269–286, 2012.

[3] J. Hetherington, A. Rodriguez-Ferran, H. Askes, The bipenalty method for arbitrary multipoint constraints. *International Journal for Numerical Methods in Engineering*, **93**, 465–482, 2013.

[4] D. Gabriel, J. Plešek, M. Ulbin, Symmetry preserving algorithm for large displacement frictionless contact by the pre-discretization penalty method. *International Journal for Numerical Methods in Engineering*, **61**, 2615–2638, 2004.

[5] P. Wriggers, *Computational contact mechanics, 2nd Eddition*. Springer, 2006.

[6] T.R. Hughes, *The finite element method: Linear static and dynamic finite element analysis*. Prentice-Hall, 1987.

[7] T. Belytschko, W.K. Liu, B. Moran, *Nonlinear finite elements for continua and structures*. John Wiley & sons, 2000.

[8] T. Belytschko, M.O. Neal, Contact-impact by the pinball algorithm with penalty and lagrangian methods. *International Journal for Numerical Methods in Engineering*, **31**, 547–572, 1991.

[9] L. Jiang, R.J. Rogers, Effects of spatial discretization on dispersion and spurious oscillations in elastic wave propagation. *International Journal for Numerical Methods in Engineering*, **29**, 1205–1218, 1990.